Superconducting strip in an oblique magnetic field

G. P. Mikitik,[1,2] E. H. Brandt,[1] and M. Indenbom[3]

[1] Max-Planck-Institut für Metallforschung, D-70506 Stuttgart, Germany
[2] B. Verkin Institute for Low Temperature Physics & Engineering,
Ukrainian Academy of Sciences, Kharkov 61103, Ukraine
[3] Institute of Solid State Physics, Chernogolovka, Russia
(Dated: February 2, 2008)

As an example for a seemingly simple but actually intricate problem, we study the Bean critical state in a superconducting strip of finite thickness d and width $2w \gg d$ placed in an oblique magnetic field. The analytical solution is obtained to leading order in the small parameter d/w. The critical state depends on how the applied magnetic field is switched on, e.g., at constant tilt angle, or first the perpendicular and then the parallel field component. For these two basic scenarios we obtain the distributions of current density and magnetic field in the critical states. In particular, we find the shapes of the flux-free core and of the lines separating regions with opposite direction of the critical currents, the detailed magnetic field lines (along the vortex lines), and both components of the magnetic moment. The component of the magnetic moment parallel to the strip plane is a nonmonotonic function of the applied magnetic field.

I. INTRODUCTION

Platelet-like type-II superconductors in a magnetic field applied at some angle θ to the normal of their plane are frequently investigated in various experiments, see, e.g., Refs. 1,2,3,4,5. However, even for the simplest case of an infinitely long strip placed in an oblique magnetic field, the critical state was theoretically studied only in the situation when the magnitude of the applied magnetic field H_a considerably exceeds the field of full-flux penetration into the sample,[3] H_p. The attempt to investigate the critical state in fields $H_a \leq H_p$ led to incorrect results,[6] since an essential feature of this state was overlooked, as will be evident from our analysis in Sec. II B.

In this paper we consider the following basic situation: A thin superconducting strip fills the space $|x| \leq w$, $|y| < \infty$, $|z| \leq d/2$ with $d \ll w$; a constant and homogeneous external magnetic field H_a is applied at an angle θ to the z axis ($H_{ax} = H_a \sin\theta$, $H_{ay} = 0$, $H_{az} = H_a \cos\theta$). It is assumed that the thickness of the strip, d, exceeds the London penetration depth, the critical current density j_c does not depend on the local induction B (Bean model[7,8]), and the lower critical field H_{c1} is sufficiently small so that we may take $B = \mu_0 H$. We consider two scenarios of switching on the external magnetic field: First, the magnitude of the external field increases from 0 to H_a at a fixed angle θ; second, one turns on H_{az} first and then H_{ax}. Interestingly, these scenarios lead to different critical states.

Taking into account the result of Ref. 9 (see also Refs. 10,11), the smallness of the parameter d/w enables us to split the two-dimensional critical state problem for the strip of finite thickness into two simpler problems: A one-dimensional problem across the thickness of the sample, and a problem for the infinitely thin strip. This splitting becomes possible since under the condition

$d/w \ll 1$ the magnetic fields and currents in the critical state essentially change along the x direction only on scales which considerably exceed the thickness d.

The solution of the critical state problem for the infinitely thin strip is known.[12,13,14] The z component of the magnetic field is completely screened by the currents flowing in the region $|x| < a$, i.e., one has $H_z = 0$ there. The length a is described by the simple formula:

$$a(h) = \frac{1}{\cosh(h \cos\theta)}. \tag{1}$$

Here and below $h \equiv H_a/H_c$, $H_c = J_c/\pi$, $J_c = j_c d$, and w is taken as the unit of length ($w = 1$). In this region of the strip, $|x| < a$, the sheet current $J(x) = \int_{-d/2}^{d/2} j(x,z)dz$ (with current density j along y) is given by

$$J(x) = -\frac{2}{\pi} J_c \arctan \frac{x\sqrt{1-a^2}}{\sqrt{a^2-x^2}}. \tag{2}$$

On the other hand, at $a < |x| < 1$ where $H_z(x) \neq 0$, one has $J = -\text{sign}(x)J_c$ with $\text{sign}(x) = \pm 1$ for $x > 0$ and $x < 0$, respectively. The explicit form of $H_z(x)$ in this region of the strip is presented in Appendix A.

In the region $|x| < a$ of the real strip (with $d \neq 0$), the flux lines are practically parallel to the planes of the strip and penetrate into the sample across its thickness from the upper and lower surfaces of the superconductor. The penetrating flux fronts form the boundary of a flux-free core, $z_\gamma(x)$, which thus consists of an upper and a lower branch. Below we consider only the upper branch since from symmetry considerations one has: $-z_\gamma^{\text{lower}}(-x) = z_\gamma^{\text{upper}}(x) \equiv z_\gamma(x)$.

Following our idea of splitting the critical state problem, we consider a small section of the strip around an arbitrary point x ($|x| < a$) as an "infinite" slab of thickness d placed in a parallel dc magnetic field H_{ax} and carrying a sheet current $J(x)$, Eq. (2). The critical state in such

a slab is well known,[13,14] and this enables us to find the flux fronts, the distribution of the magnetic fields, and the currents across the thickness of the strip in the region $|x| < a$. Since the critical state in the slab depends on how H_{ax} and J was turned on, the above-mentioned dependence of the critical state in the strip on the prehistory of H_{ax} and of H_{az} appears. Of course, a similar procedure may be used in the region $a < |x| < 1$ to find the distribution of the magnetic fields, but there the appropriate analysis is trivial since $j(x, z)$ is constant; we thus do not discuss it below.

II. MAGNETIC FIELD IS INCREASED AT CONSTANT TILT ANGLE

In the case of the first scenario of switching on the magnetic field when θ =const and h has increased monotonically, it is convenient to introduce the function,

$$F(x, h) \equiv \frac{2}{\pi} \left[h \sin \theta - \arctan \frac{x\sqrt{1 - a(h)^2}}{\sqrt{a(h)^2 - x^2}} \right], \qquad (3)$$

which is proportional to the x component of the magnetic field on the upper surface of the strip at $|x| \le a$, $H_{us}(x) = H_{ax} + 0.5J(x) = (J_c/2)F(x, h)$. Below we shall also use the two characteristic fields:

$$h_p = \frac{\pi}{2 \sin \theta}, \qquad (4)$$

and h_f defined by the equations:

$$h_f = h_p - u + \frac{\arctan[\tan \theta \, \mathrm{th}(u \cos \theta)]}{\sin \theta},$$
$$\cosh(u \cos \theta) = \sin \theta \cosh(h_f \cos \theta), \qquad (5)$$

where u is some parameter. The meaning of these fields will become clear below.

A. Interval $0 < h < h_f$

Consider first the flux front in the interval $0 < h < h_f$. It is essential that there exists a point on the upper plane of the strip where the derivative $dH_{us}(x)/dx$ vanishes. A simple calculation gives that this occurs at the point with the coordinate x_1,

$$x_1(h) = a(h) \sin \theta. \qquad (6)$$

Thus, when h increases, the flux lines at $-a(h) < x < x_1(h)$ monotonically penetrate into the strip through its upper surface, and the shape of the core in this interval of x is determined by the equation:

$$z_\gamma(x) = (d/2)[1 - F(x, h)]. \qquad (7)$$

This formula follows from the well-known distribution of the magnetic field in the "slab" shown in Fig. 1

("Bean profiles"). On the other hand, in the interval $x_1(h) < x < x_0(h)$ the flux lines *leave* the sample, and at $x > x_0$ vortices of opposite sign penetrate into the strip, Fig. 1. Here the point $x_0(h)$ is found from the condition $H_{us}(x_0) = 0$, i.e., from

$$F(x_0, h) = 0. \qquad (8)$$

It is clear from the inspection of Fig. 1 that in the interval $x_1(h) < x < x_2(h)$ the shape of the core is determined by the flux front occurring at the field h_* which has to be found from the equation

$$x = a(h_*) \sin \theta. \qquad (9)$$

Thus, in this interval one has

$$z_\gamma(x) = (d/2)[1 - F(x, h_*)]. \qquad (10)$$

In the same interval there is also a front $z_1(x)$ separating the regions of the strip with opposite signs of the critical current density, see Figs. 1, 2. This front is described by the formula:

$$z_1(x) = (d/4)[2 + F(x, h) - F(x, h_*)]. \qquad (11)$$

At the point $x_2(h)$ the front $z_1(x)$ reaches the boundary of the core $z_\gamma(x)$, and hence, this $x_2(h)$ is determined by the condition $z_\gamma(x_2) = z_1(x_2)$. Using formulas (9)-(11), one then obtains for x_2:

$$x_2 = a(u) \sin \theta,$$
$$F(x_2, h) + F(x_2, u) = 0. \qquad (12)$$

At $x_2(h) < x < a(h)$ the critical current density has only negative sign, $j = -j_c$, at $z > z_\gamma$, and we arrive at

$$z_\gamma(x) = (d/2)[1 + F(x, h)]. \qquad (13)$$

We see that in the interval of the magnetic fields $0 < h < h_f$ the width of the flux-free core is equal to $2a(h)$, but its size along z is less than d, see Fig. 2. When $h \to h_f$, the difference $a(h) - x_2(h)$ tends to zero, and at $h = h_f$ one has $x_2(h) = a(h)$. With the use of Eqs. (1) and (12) this condition may be rewritten as Eqs. (5).

B. Interval $h_f < h < h_p$

When $h_f < h < h_p$, the upper and the lower branches of the flux-free core merge in the intervals $x_3 < |x| < a$, and hence the size of the flux-free core in the x direction, $2x_3(h)$, becomes less than $2a(h)$, see Figs. 3, 4. Here $x_3(h)$, which lies between $x_1(h)$ and $a(h)$, is determined by the condition, $z_\gamma^{\mathrm{upper}}(x_3) = z_\gamma^{\mathrm{lower}}(x_3)$, or in the explicit form by the equations:

$$x_3 = a(u) \sin \theta,$$
$$F(-x_3, h) + F(x_3, u) = 2, \qquad (14)$$
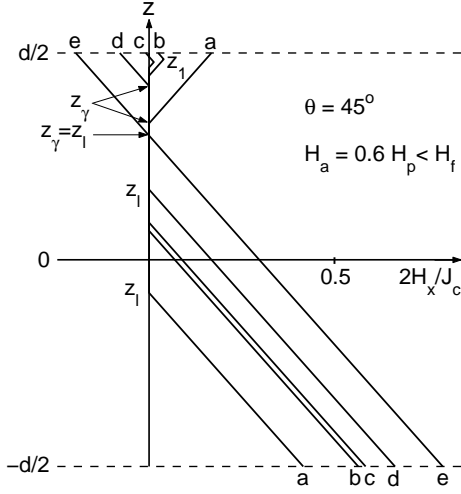
FIG. 1: Bean profiles of the magnetic field $H_x(z)$ across the strip at 5 positions x in the strip at $h < h_f$. Here $\theta = 45°$, $H_a = 0.6H_p < H_f = 0.834H_p$, thus $x_1 = 0.478$, $x_0 = 0.597$, $x_2 = 0.617$, $a = 0.677$ in units w (see Fig. 6). The characteristic z values $z_\gamma(x)$, $z_l(x) = -z_\gamma(-x)$, and $z_1(x)$ are defined in the text and in Fig. 2. Shown are: a) $0 < x = 0.35 < x_1$, b) $x_1 < x = 0.57 < x_0$, c) $x_0 < x = 0.61 < x_2$, d) $x_2 < x = 0.65 < a$, e) $x \geq a = 0.677$. For all these profiles, $2H_x/J_c$ is $F(x,h)$ on the upper surface, and $F(-x,h)$ on the lower surface. The continuation of the increasing parts of the profiles b) and c) intersects the upper surface at $F(x,h_*)$.

where we have taken into account the symmetry of the flux-free core and formulas (7), (9), (10). In other words, we find that not only the z-size of the core is less than d, but also its x-size is less than the width of the region in the strip, $2a(h)$, where $H_z = 0$. In the interval $-x_3(h) < x < x_1(h)$, the core is again described by Eq. (7), while in the interval $x_1(h) < x < x_3(h)$ it is given by Eqs. (9), (10). When h becomes equal to h_p defined by formula (4), the point x_3 reaches x_1, and moreover, the core disappears at all since at this field the difference $z_\gamma^{\text{upper}}(x) - z_\gamma^{\text{lower}}(x)$ vanishes even for $|x| < x_1$. Thus, $h_p = 0.5\pi/\sin\theta$ is the field of full penetration of flux into the strip in the oblique magnetic field. This field has a simple meaning. In usual units one finds for the x component of the penetration field, $H_c h_p \sin\theta = J_c/2$, i.e., the penetration occurs when the x component of the applied field has completely penetrated into the slab.

Interestingly, the part of the boundary of the core in the interval $x_1(h) < x < x_3(h)$, as well as its part in the interval $x_1(h) < x < x_2(h)$ for the fields $0 < h < h_f$, is described by a universal function of z on x which does not depend on h at all, see Eqs. (9), (10). The upper corner of the core, i.e., the point $x_2(h)$ for $0 < h < h_f$ or the point $x_3(h)$ for $h_f < h < h_p$, moves just along the line described by this function when h increases, Fig. 5.

As to the front separating the regions of the strip with opposite signs of the critical current density, it is still described by Eq. (11) in the region $x_1 < x < a$ even for
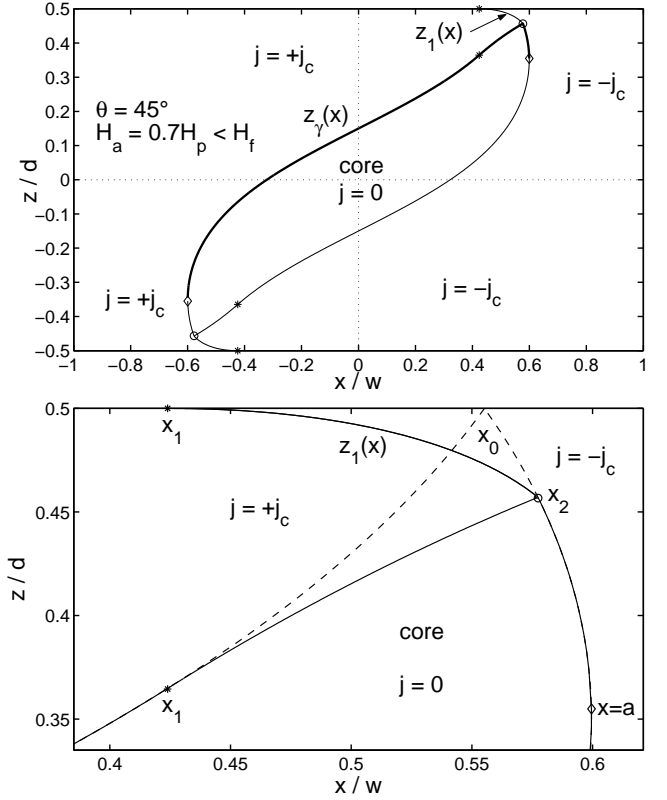

FIG. 2: The flux and current fronts in a thin strip in an increasing magnetic field H_a that is inclined by a constant angle $\theta = 45°$ away from the normal of the strip plane. Shown is the state when $H_a = 0.7H_p < H_f = 0.834H_p$ where $H_p = (J_c/2)/\sin\theta$ is the field of full penetration, see text. The current-free core is delimited by the functions $z_\gamma(x)$ (bold line) and $-z_\gamma(-x)$. The current density to the left of this core and of the "tails" $z_1(x)$, $-z_1(-x)$, is $j = j_c$, and to the right $j = -j_c$. The lower plot enlarges the region near the points $x = x_1$, $x = x_2$, and $x = a$ on these curves, see text. The two dashed lines are extensions of the fronts depicted in the regions $-a \leq x \leq x_1$ and $x_2 \leq x \leq a$ and cut the upper surface $z = d/2$ at the point $x = x_0$ where the local H_x vanishes, Eq. (8).

$h_f < h < h_p$. However, in the interval $x_3 \leq x \leq a$, apart from this upper branch of the front, $z_1(x)$, a lower branch $z_2(x)$ appears, and these branches join each other with vertical slope at $x = a(h)$, Fig. 4. Knowing the upper branch, one can find the lower branch from the given value of the sheet current $J(x)$, Eq. (2), yielding

$$z_2(x) = (d/4)[F(-x,h) - F(x,h_*)], \qquad (15)$$

where $h_*(x)$ is found from

$$x = a(h_*)\sin\theta.$$

A complete set of flux and current fronts is shown in Fig. 6 for three tilt angles $\theta = 30°$, $45°$, and $60°$. Note that when H_a increases, not only does the flux-free core
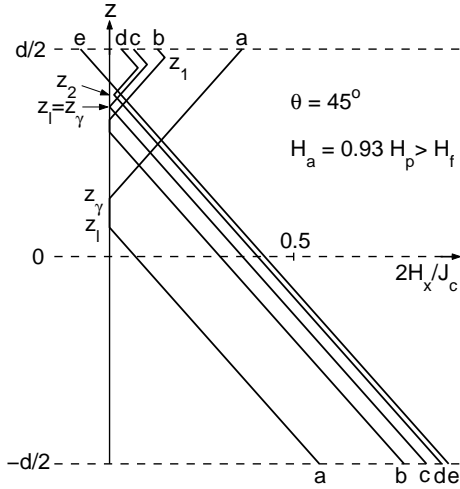
FIG. 3: Bean profiles of the magnetic field $H_x(z)$ across the same strip as in Fig. 1 but for higher applied field $h > h_f$, $H_a = 0.93H_p > H_f = 0.834H_p$, thus $x_1 = 0.311$, $x_3 = 0.422$, $x_0 = 0.438$, $a = 0.440$ in units w (see Fig. 4). The characteristic z values $z_\gamma(x)$, $z_l(x) = -z_\gamma(-x)$, $z_1(x)$, and $z_2(x)$ are defined in the text and in Fig. 4. Shown are the 5 profiles: a) $0 < x = 0.15 < x_1$, b) $x_1 < x = 0.40 < x_3$, c) $x = x_3 = 0.422$, d) $x_3 < x = 0.43 < a$, e) $x \geq a = 0.440$. Profile d) does not cut the field-free core and has $H_x(z) > 0$ everywhere. The values of H_x on the upper and lower surfaces are given by the same expressions $F(x,h)$ and $F(-x,h)$ as in Fig. 1.

shrink but also the current front separating the regions with $j = \pm j_c$ shifts in the sample. In other words, the current distribution changes not only near the core but also in the region away from it. This result disproves the main assumption of Ref. 6 that the currents can change only at the flux front but the critical currents remain unchanged in the regions penetrated by flux lines. In Ref. 6 the flux fronts in inclined field are thus incorrect.

C. Region $h > h_p$

Although at $h > h_p$ the z component of the magnetic field does not penetrate into the region $|x| \leq a(h)$ of the strip, its x component completely penetrates into the sample, and the flux-free core is absent, Fig. 7. The two branches of the boundary separating the regions of the strip with opposite signs of the critical current density are still described by Eqs. (11) and (15) in the interval $x_1 < x < a$. In the interval $|x| < x_1$ only one of these branches exists, which is the continuation of the $z_2(x)$ and is described by the formula:

$$z_2(x) = \frac{d}{\pi} \arctan\frac{x\sqrt{1-a^2}}{\sqrt{a^2-x^2}}$$
$$= \frac{d}{4}\left[F(-x,h) - F(x,h)\right]. \qquad (16)$$

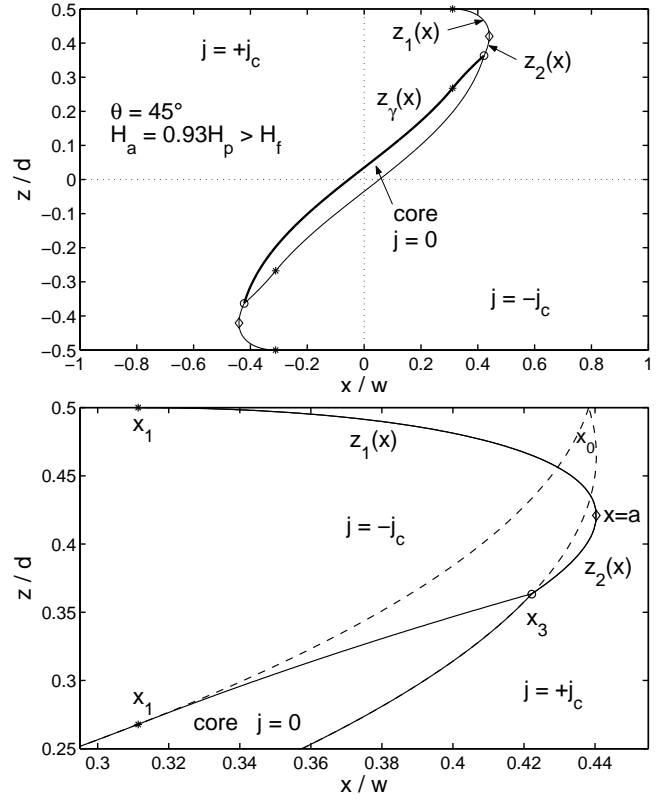FIG. 4: The fronts as in Fig. 2 but at a larger field $H_a = 0.93H_p > H_f$. As in Fig. 2 the flux-free core is formed by the curves $z_\gamma(x)$, $-z_\gamma(-x)$, but the tail separating regions with $j = \pm j_c$ is now composed of two functions $z_1(x)$ and $z_2(x)$, which join vertically at $x = a$ and reach the core at $x = x_3$.

This formula follows from the given value of the sheet current $J(x)$, Eq. (2).

Interestingly, even at high magnetic fields $h \gg h_p$ the current front is S-shaped and does not tend to a straight line as it was assumed in Ref. 3. Probably, it is for this reason that there is a disagreement between the theoretical and experimental results in Ref. 3 at $\theta \sim \pi/2$. However, it is necessary to keep in mind the following: Our approximation based on the splitting procedure is valid if $dz_\gamma/dx \ll 1$ and $dz_{1,2}/dx \ll 1$. These inequalities are fulfilled almost everywhere in the strip when the characteristic scales in the x direction (i.e., x_1, and $a-x_1$) considerably exceed the thickness d. Thus, the region $h > h_p$ may be considered within our approximation only when $(\pi/2)\cot\theta < \ln(2ew/d)$, i.e., when the angle θ is not too small, see inset in Fig. 7. Otherwise, the component H_z completely penetrates into the sample at lower H_a than the component H_x does. In this case the field of full penetration is $H_p^\perp/\cos\theta$ where $H_p^\perp = (J_c/\pi)\ln(2ew/d)$ is the penetration field at $\theta = 0$,[15] and the current fronts will differ from those shown in Fig. 7. Note that the angular dependence of the true penetration field is given by $H_p(\theta) = \min(H_p^\perp/\cos\theta,\ J_c/2\sin\theta)$ and is a nonmono-
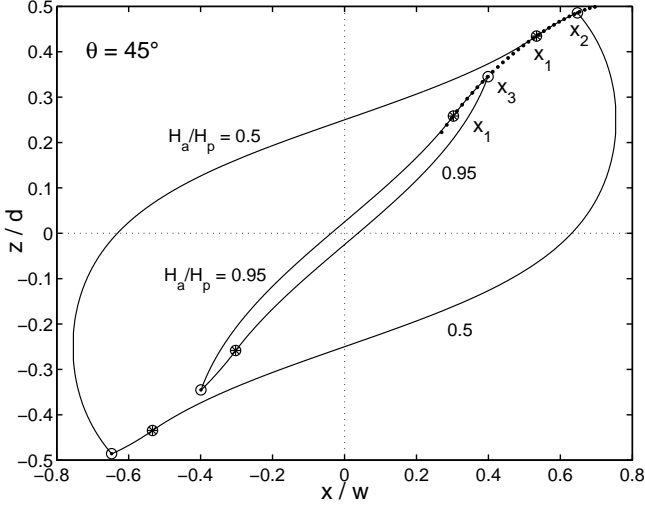

FIG. 5: Two flux-free cores in a thin strip in increasing magnetic field H_a inclined by $\theta = 45^\circ$ as in Figs. 2, 4. The bold dotted line shows the universal curve, Eqs. (9,10), on which the upper part $x_1 \le x \le x_2$ or x_3 of all flux fronts lies when $H_a \le H_p$, see text. The depicted cores belong to $H_a/H_p = 0.5$ and $H_a/H_p = 0.95$. The circles mark the characteristic points x_1, x_2, and x_3 on the fronts.

tonic function, see inset in Fig. 7.

III. MAGNETIC FIELD COMPONENTS ARE SWITCHED ON SUCCESSIVELY

Consider now the scenario when the field H_{az} is switched on first and then one switches on H_{ax}. The resulting magnetic field again is $H_{ax} = H_a \sin\theta$, $H_{ay} = 0$, $H_{az} = H_a \cos\theta$. In this case the analysis of the critical state is quite similar to that presented in the Sec. II, and we present only the results here.

The field of full penetration of flux is still described by formula (4). However, at any $h \le h_p$ the x size of the flux-free core, $2a_1$, is less than the width $2a = 2/\cosh(h\cos\theta)$ of the region where $H_z = 0$. This a_1 is determined by the formula $J(a_1) = H_{ax} - J_c$, or explicitly, by

$$a_1 = \frac{a\cos(h_x/2)}{\left[1 - a^2 \sin^2(h_x/2)\right]^{1/2}}, \quad (17)$$

where $h_x = h\sin\theta = H_{ax}/H_c$. One more characteristic scale is $\tilde{x}_1(h)$ determined by the relation: $J(\tilde{x}_1) = -H_{ax}$, which leads to the explicit expression for $\tilde{x}_1$:

$$\tilde{x}_1 = \frac{a\sin(h_x/2)}{\left[1 - a^2 \cos^2(h_x/2)\right]^{1/2}}. \quad (18)$$

In the interval $-a_1 \le x \le \tilde{x}_1$ the shape of the flux-free core is described by formula (7). But in the region
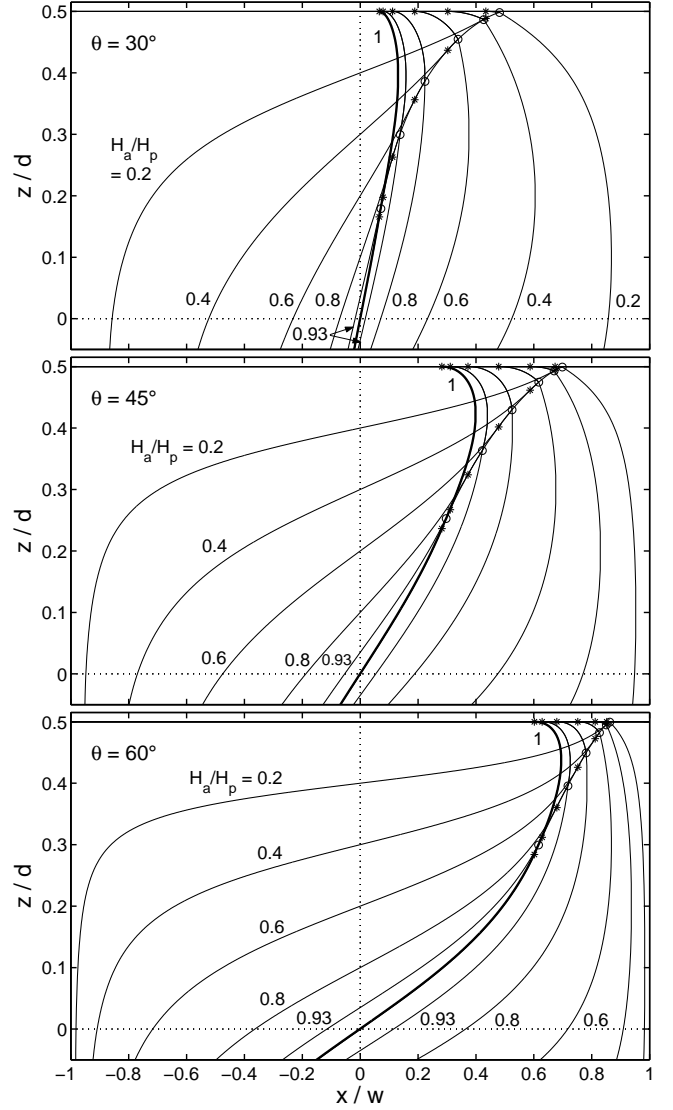

FIG. 6: Flux and current fronts in a thin strip in an increasing magnetic field H_a inclined by three angles $\theta = 30^\circ$, $\theta = 45^\circ$, and $\theta = 60^\circ$ away from the strip normal. Shown are the complete fronts for six fields $H_a/H_p = 0.2$, 0.4, 0.6, 0.8, 0.93, and 1 (bold line), where $H_p = (J_c/2)/\sin\theta$, see also Figs. 1-5.

$\tilde{x}_1 \le x \le a_1$ one has

$$z_\gamma(x) = \frac{d}{2}\left[1 - \frac{2}{\pi}\arctan\frac{x\sqrt{1-a^2}}{\sqrt{a^2 - x^2}}\right]. \quad (19)$$

In this interval of x there is also a boundary $z_3(x)$ separating the regions of the strip with opposite directions of j_c, see Fig. 8. This horizontal line is described by

$$z_3(x) = \frac{d}{2}\left[1 - \frac{h_x}{\pi}\right]. \quad (20)$$

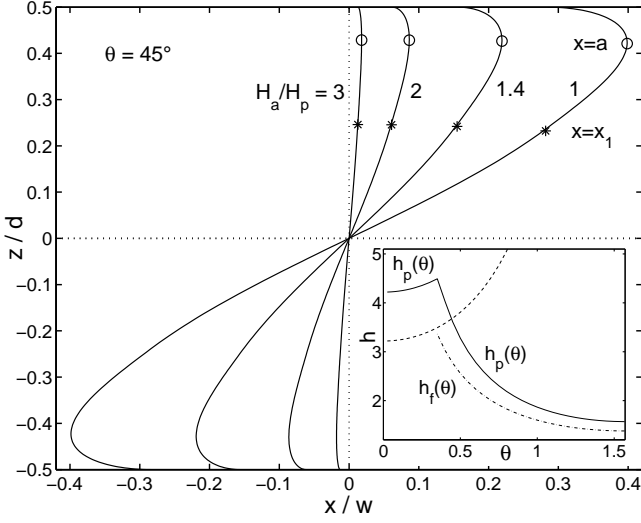This boundary continues in the region $a_1 \le x \le a$ where

FIG. 7: The current fronts separating the regions with critical currents of opposite direction in a thin strip in increasing magnetic field H_a inclined by $\theta = 45°$. At the depicted fields $H_a/H_p = 1, 1.4, 2, 3$ *above* the penetration field $H_p = (J_c/2)/\sin\theta$, the flux-free core has collapsed into one line, and the front is composed of the three curves $z_2(0 \leq x \leq x_1)$ [Eq. (16)], $z_2(x_1 \leq x \leq a)$ [lower branch, Eq. (15)], and $z_1(a \geq x \geq x_1)$ [upper branch, Eq. (11)]. Note that even at large H_a these front lines *are not straight lines* as it might be expected. At $a \ll w$ these fronts collapse into one curve when plotted versus x/a. Inset: the dashed line $h \sim \ln(2ew/d)/\cos\theta$ schematically shows the boundary above which our splitting procedure fails, see Sec. II C. The solid line gives the penetration field $h_p(\theta) \equiv \pi H_p/J_c = \min[\ln(2ew/d)/\cos\theta, 0.5\pi/\sin\theta]$ and the dash-dotted line shows $h_f(\theta)$, Eq. (5).
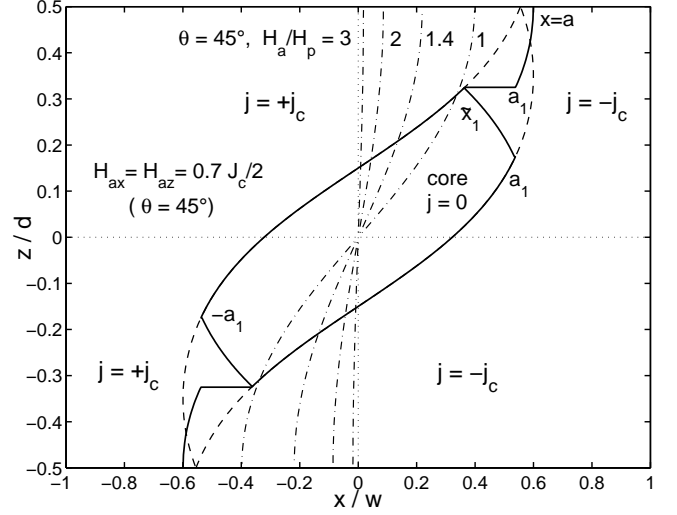

FIG. 8: Current and flux fronts in a thin strip to which first the perpendicular magnetic field H_{az} is applied and then the in-plane component H_{ax} is increased from zero to $H_{ax} = H_{az} = 0.7J_c/2$, resulting in a final tilt angle $\theta = 45°$ (scenario 2, Sec. III). The solid line z_γ from $x = -a_1$ via $\tilde{x}_1$, a_1, $-\tilde{x}_1$ to $-a_1$ forms a flux-free core. This core is connected to the surfaces by tails composed of a horizontal part $z_3(\tilde{x}_1 \leq x \leq a_1)$, and a curved part $z_3(a_1 \leq x \leq a)$, ending at the point $(a, d/2)$. The dashed lines give the extensions of the fronts which exactly coincide with the dashed lines shown in Fig. 2 and end at x_0. The dash-dotted lines are the current fronts of this scenario above full penetration, at the same fields as in Fig. 7 for $\theta = 45°$. Note that these fronts are *monotonic*, while the corresponding fronts of scenario 1 in Fig. 7 are S-shaped.

it is given by an expression coinciding with Eq. (16):

$$z_3(x) = \frac{d}{\pi} \arctan\frac{x\sqrt{1-a^2}}{\sqrt{a^2-x^2}}. \qquad (21)$$

When h approaches h_p, the point a_1 tends to $\tilde{x}_1$, and the difference $z_\gamma^{\text{upper}}(x) - z_\gamma^{\text{lower}}(x)$ vanishes simultaneously for all $|x| \leq \tilde{x}_1$. At $h = h_p$ the flux-free core disappears, while the boundary $z_3(x)$ exists at $h \geq h_p$, and it is described by the expression (21) in the whole interval $-a \leq x \leq a$, see Figs. 8, 9. When $H_{ax} \geq J_c/2$ is increased further, this saturated current front does not change any more.

Thus, we see that the shape of the flux-free core and the boundary between the regions with opposite directions of the critical current density do not coincide with those described in Sec. II and thus depend on the magnetic history.

IV. MAGNETIC FIELD LINES

Using the obtained results, it is easy to find the distribution of the magnetic fields in the critical state of the strip. One may either integrate over the current-carrying area, noting that each current path has the magnetic field of a straight wire (Fig. 10). Or one may derive analytical expressions using our splitting approximation (Fig. 11). The z component, $H_z(x)$, in this approximation does not depend on z and is given by the formulas of Refs. 12,13,14 [or by Eq. (A8) in compact form], and the x component is

$$H_x(x,z) = H_x(x,-d/2) + \int_{-d/2}^{z} j_y(x,z')dz', \qquad (22)$$

where $H_x(x,-d/2)$ is the field on the lower surface of the strip. At $|x| \leq a$ one has $H_x(x,-d/2) = (J_c/2)F(-x,h)$, while $H_x(x,-d/2) = H_a\sin\theta + (J_c/2)\text{sign}(x)$ at $a \leq |x| \leq 1$. Taking into account that $j_y(x,z)$ has only the values j_c, $-j_c$, or 0, and knowing $z_\gamma(x)$ and the boundaries between the regions with $\pm j_c$, one can easily calculate $H_x(x,z)$ everywhere in the strip and near the strip explicitly.

As an example, Figs. 10 and 11 show the magnetic field lines (parallel to the Abrikosov vortex lines) in the strip and near the strip for the first scenario of switching on the magnetic field at constant tilt angle θ till $H_a = 0.7H_p$ is reached. Both figures show the field lines obtained as
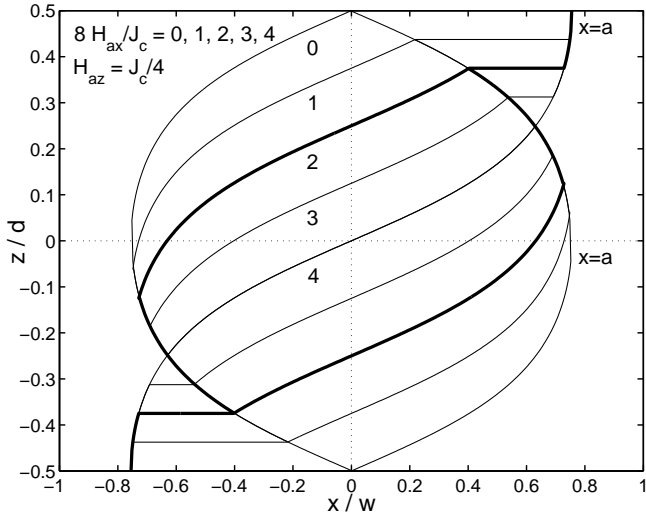
FIG. 9: The flux and current fronts in a thin strip in which first $H_{az} = J_c/4$ is applied and then H_{ax} is increased from zero to full penetration, $8H_{ax}/J_c = 0, 1, 2, 3, 4$ (scenario 2, Sec. III). The complete front for $H_{ax} = J_c/4$ is depicted as bold line, see also Fig. 8. The front 4 through the strip center $(0, 0)$ applies to all $H_{ax} \geq J_c/2$ and depends only on H_{az}. Note that the depicted fronts correspond to different tilt angles θ, e.g., the saturated front corresponds to $\theta = \arctan(H_{ax}/H_{az}) \geq \arctan 2 \approx 63°$.

contour lines of the vector potential $A_y(x, z)$ related to $\mathbf{H}(x, z) = \nabla \times (\hat{\mathbf{y}} A_y)$. Figure 10 depicts the field lines calculated directly from Ampère's law using the currents obtained in Sec. II A and formula (A1) of Appendix A at $d/w = 0.08$. It is important that this current distribution indeed leads to a flux-free core which is close to that obtained in Sec. II A. On the other hand, figure 11 uses expressions (A2) - (A8) of Appendix A for the same $d/w = 0.08$. These expressions were derived with our splitting procedure. It can be seen that the agreement of both field-line patterns is good, but the fine details near the current fronts can be more easily resolved in Fig. 11 (top) which is based on the simple analytical formulas. In particular one can see that the field lines exactly flow around the core in which $j = 0$, and some field lines cut the line ("tail") that separates regions with $j_y = \pm j_c$ and runs from $x = x_1$ on the upper surface to the cusp of the core at $x = x_2$, see also Fig. 2. The slight wiggle of the field lines occurring near $|x| = a$ in Fig. 11 (bottom) is an artifact, since the condition for the splitting procedure, $dz_\gamma/dx \ll 1$, fails at this point. However, a more detailed analysis shows that the difference between the field-line patterns of Figs. 10 and 11 manifests itself only in narrow intervals near $x = \pm a$.
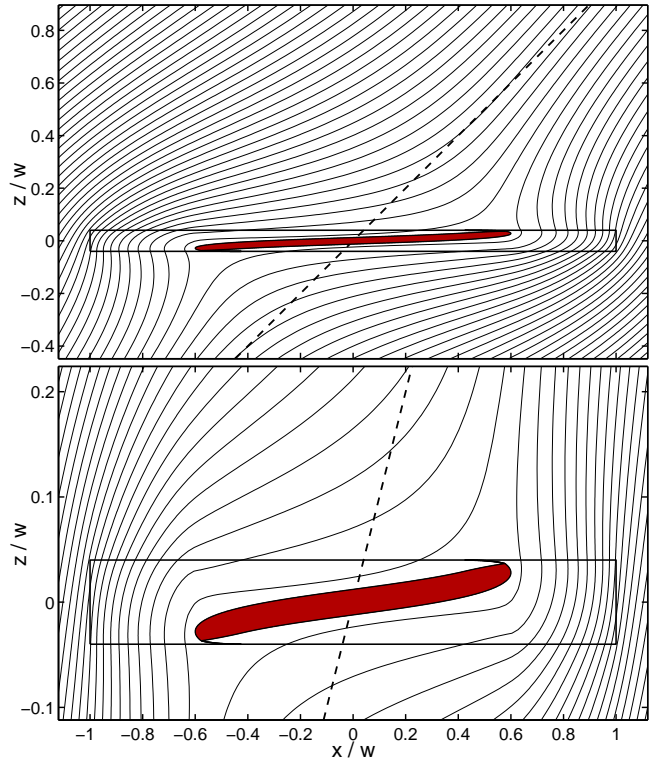

FIG. 10: The magnetic field lines for a strip of width $2w$ and thickness $d = 0.08w$ in an applied field inclined by $\theta = 45°$ and increased from zero to $H_a = 0.7H_p$ as in Fig. 2 (scenario 1). These field lines were computed as equidistant contour lines of the vector potential $A_y(x, z)$, Eq. (A1), yielding a density of lines proportional to the local magnetic field $H(x, z)$. The gray area shows the current and field-free core. The dashed line is along H_a. The upper plot is to scale, the lower plot is stretched along z by a factor of 4.

V. MAGNETIC MOMENT

In an oblique magnetic field, apart from the z component of the magnetic moment of the strip, M_z, an x component M_x appears, and both can be investigated experimentally.[3] The expression for M_z (per unit length along y) is known:[13]

$$m_z \equiv -\frac{M_z}{J_c w^2} = \tanh(h \cos \theta). \tag{23}$$

Knowing $z_\gamma(x)$ and the boundaries between the regions with opposite signs of the critical current density, given in Secs. II and III, one can calculate M_x for the strip from the formula:

$$M_x = -\int_{-a}^{a} dx \int_{-d/2}^{d/2} z j_y(x, z) dz. \tag{24}$$

Here M_x is given per unit length along y, and we have taken into account that only the region of the strip, $|x| \leq a$, gives a nonzero contribution to M_x. The saturation
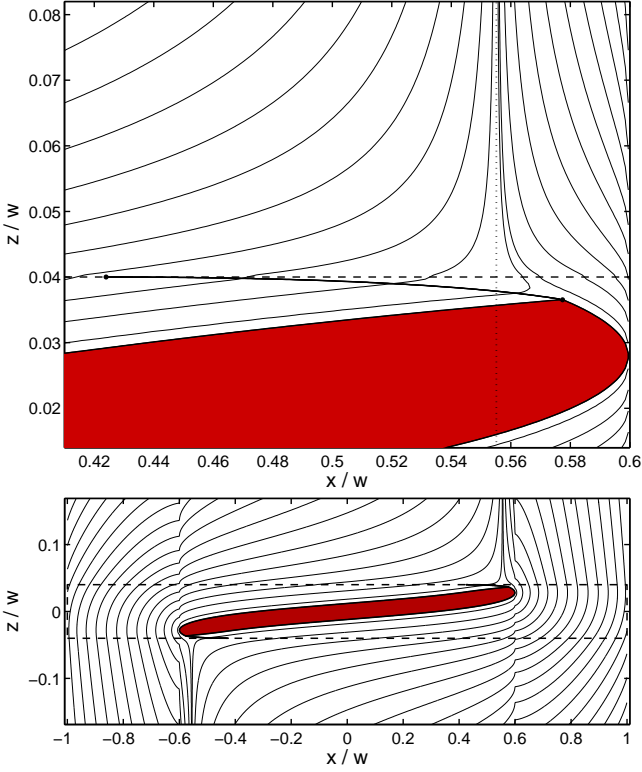
FIG. 11: The magnetic field lines for the same strip as in Fig. 10 ($d = 0.08w$, $\theta = 45°$, $H_a = 0.7H_p$) from Eqs. (A2)-(A7). To reveal the details near the current fronts, the field lines here are nonequidistant contour lines of the analytic vector potential $A_y(x,y)$ of Appendix A, with levels $A_\nu \propto \nu^2 \text{sign}(\nu)$, $\nu = 0, \pm 1, \pm 2, \ldots$, yielding more lines at low fields. The gray area shows the current and field-free core. The dashed line marks the surface of the strip and the dotted line shows $x = x_0$, Eq. (8), defined by $H_x(x_0, d/2) = 0$. Note that field lines cut the line (from $x = x_1$ to $x = x_2$ marked by bold dots) that separates regions with $j_y = \pm j_c$. The lower plot shows the same case on different x and z scales.

value of M_x, which is achieved in high fields for $\theta = \pi/2$, is $M_x^{\text{sat}} = -J_c dw/2$, see Appendix B.

It is known for the infinitely thin strip[16] that whatever its length in y, the ends of the strip (in y) always give the same contribution to M_z as that caused by the currents j_y flowing in the y direction. When M_x is calculated, it is necessary to allow for the fact that near the ends of the strip the currents may have not only y and z components but also an x component, i.e., the problem becomes three dimensional. However, using the conservation law for the current, $\text{div} \mathbf{j} = 0$, one can show that even in this three dimensional case the ends of the strip strictly double M_x. It is for this reason that the factor $1/2$ was omitted in formula (24).

In Fig. 12 we compare the H_a-dependences of M_x for the two scenarios of switching on the magnetic field. Note that $M_x^{(2)}(H_a)$ of scenario 2 is always larger than $M_x^{(1)}(H_a)$ of scenario 1, except for the trivial angles
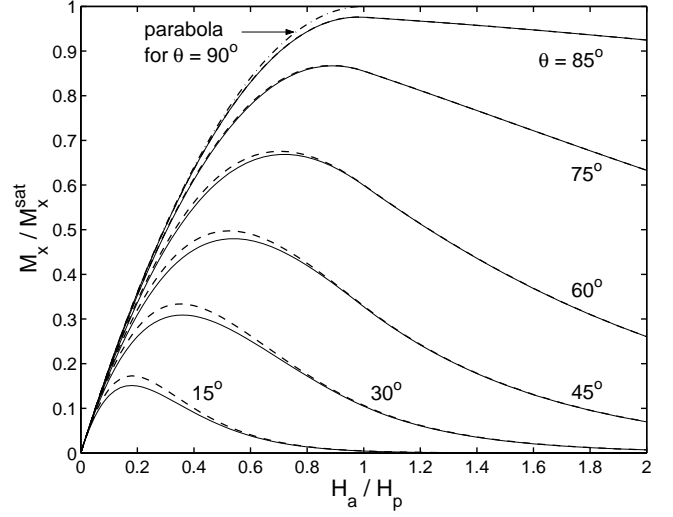

FIG. 12: Magnetic-moment component $M_x(H_a)/M_x^{\text{sat}}$ from Eq. (24) and Appendix B, for scenario 1 (solid lines) and scenario 2 (dashed lines) plotted versus the applied magnetic field H_a in units of the penetration field $H_p = J_c/2 \sin \theta$ for tilt angles $\theta = 15°$, $30°$, $45°$, $60°$, $75°$, and $85°$. Here $M_x^{\text{sat}} = -J_c dw/2$. The dot-dashed parabola $M_x/M_x^{\text{sat}} = 1 - (1 - H_a/H_p)^2$ applies to $\theta = 90°$ (H_a along x), and for $\theta = 0$ (H_a along z) one has $M_x = 0$. For all other angles the $|M_x(H_a)|$ for scenario 2 is larger than for scenario 1.

$\theta = 0$ where $M_x = 0$, and $\theta = \pi/2$ where $M_x/M_x^{\text{sat}} = 1 - (1 - H_a/H_p)^2$. All $M_x(H_a)$ exhibit a maximum of height $M_x^{\text{max}}/M_x^{\text{sat}} \approx 2\theta/\pi$ occurring at $H_a/H_p \approx 2\theta/\pi$, and they have the same slope $\partial M_x/\partial H_a = 2M_x^{\text{sat}}/H_p$ at $H_a = 0$. The difference $M_x^{(2)} - M_x^{(1)}$ is also maximum near H_p, see the dashed curve in Fig. 13. Figure 13 plots the $M_x^{(1)}$ of scenario 1 as in Fig. 12 but with both abscissa and ordinate stretched by a factor $\pi/(2\theta) \geq 1$ such that the approximate scaling of the $M_x^{(1)}(H_a)$ at not too large H_a/H_p is seen. The $M_x^{(2)}(H_a)$ curves of scenario 2 scale even better.

The nonmonotonic dependence of M_x on H_a can be understood from the following arguments: In the region $|x| < a$ the x component of the external magnetic field, $H_{ax} = H_a \sin \theta$, leads to an asymmetric distribution of the currents over z, see Figs. 1-9. It is this asymmetry that generates the M_x component. Thus, M_x can be estimated as follows: $M_x \sim M_x^{\text{sat}} \cdot (a/w)(H_a/H_p)$. The factor a/w decreases with H_a, see Eq. (1), and its product with the increasing factor H_a/H_p leads to the observed nonmonotonic behavior of $M_x(H_a)$.

VI. CONCLUSIONS

We solve the critical state problem for a strip of finite thickness in an oblique magnetic field. Two scenarios of switching on the external magnetic field are considered:
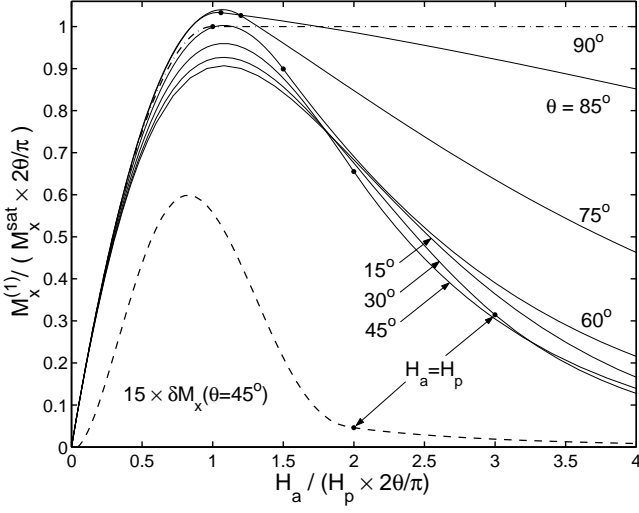
FIG. 13: The same magnetization curves as in Fig. 12 for scenario 1, plotted as $M_x/(M_x^{\text{sat}} \times 2\theta/\pi)$ versus $H_a/(H_p \times 2\theta/\pi)$. The dots mark the point where $H_a = H_p$. The dot-dashed curve gives the limit $\theta = 90°$. The dashed line shows the difference of the M_x of scenarios 2 and 1 for $\theta = 45°$ in form of $15 \times (M_x^{(2)} - M_x^{(1)})/(M_x^{\text{sat}} \times 2\theta/\pi)$.

(1) the magnetic field is increased at a constant tilt angle θ, and (2) the magnetic field components are switched on successively. The resulting critical states are different in these two cases, *even after the flux has fully penetrated the strip.*

Another characteristic feature of both states is that, below the field of full penetration, the height of the flux-free core is *less* than the strip thickness, i.e., the core does not reach the flat surfaces but is connected to them by lines ("tails") that separate regions with opposite direction of the critical currents.[17] Moreover, the width of the core may be narrower than the region of the strip in which the z component of the magnetic field (i.e., the component perpendicular to the plane of the strip) vanishes.

One more interesting feature of the critical states in strips in an oblique magnetic field follows from the data of Figs. 6 and 9: When the applied field increases, and hence the flux lines further penetrate into the sample, the current distribution changes not only near the flux front but also away from it, i.e., in the regions where the critical state was established before. Note that this feature is also seen in figures of Ref. 18 in which the critical state of a rotating cylinder was considered in magnetic fields perpendicular to its axis. These findings mean that this property of the current distributions in the critical states is characteristic of the general case when the geometry of experiment is not too symmetric, while the usual change of currents at the penetrating flux front occurs only in special symmetric situations (e.g., when the tilt angle $\theta = 0$, $\pi/2$, or when the cylinder does not rotate). Finally, we found the somewhat unexpected result that in an oblique

magnetic field H_a exceeding the penetration field, the current front separating the regions of the strip with $\pm j_c$ generally is *not a straight line* and can shift in the sample when H_a is increased further.

The above general features of the critical sate are robust and hold even if the strip is not very thin or if its cross section is not rectangular, i.e., these features are common for all critical states in *nonsymmetric* situations. However, the fine details of our results (e.g., the short tail from x_1 to x_2 in Fig. 2) require that all characteristic lengths in the plane of the strip considerably exceed its thickness. If some length of the flux-free core does not satisfy this condition, one may expect deviations from the presented results in this region of the core. Furthermore, the temperature should be low enough that flux creep does not smear these details, i.e., the creep exponent n in the current–voltage law $E(j) \propto (j/j_c)^n$ should be large. A detailed numerical investigation of the effect of flux creep is under way. Note that the detailed shape of the flux-free core and of the boundaries between regions with opposite critical current in principle can be investigated via the in-plane component of the magnetic moment, while it has little influence on the magnetic field on the surface.

APPENDIX A: VECTOR POTENTIAL

The magnetic field lines of a strip parallel to y coincide with the contour lines of the vector potential $A_y(x,z)$ related to the current density $j_y(x,z)$ by $\nabla^2 A_y = -j_y$ or

$$A_y(\mathbf{r}) = \int d^2r'\, j_y(\mathbf{r}') \frac{\ln|\mathbf{r} - \mathbf{r}'|}{2\pi}, \qquad (A1)$$

with $\mathbf{r} = (x,z)$.

For the special case of a thin strip in an oblique applied field, we can also find $A_y(x,z)$ using our splitting procedure. Here, as an example, we give the expressions for A_y in the case of scenario 1 at $h \leq h_f$ (see Fig. 2). Inside the core delimited by the two lines $z_\gamma(x)$ and $-z_\gamma(-x)$, one has $H_x = H_z = j_y = 0$, and we may put $A_y = 0$ there. Within the core width ($|x| < a$) one obtains:

$$A_y(x,z) = -\int_{z_\gamma(x)}^{z} H_x(x,z')\, dz'. \qquad (A2)$$

Inserting the H_x from Sec. IV into Eq. (A2), one finds explicit formulas for A_y. Equivalently, the A_y inside the core width can be calculated directly from the equation $\partial^2 A_y/\partial z^2 = -j_y$ and the current density of Sec. II. Eventually, we obtain the following expressions for $A_y =$

$(j_c/2)\,a_y(x,z)$, depending on a, x_1, x_2, $z_\gamma(x)$, and $z_1(x)$: For $-a < x < x_1$, $z_\gamma < z < d/2$ and for $x_1 < x < x_2$, $z_\gamma < z < z_1$:

$$a_y = 2A_y/j_c = -(z - z_\gamma)^2\,, \qquad (A3)$$

for $x_1 < x < x_2$, $z_1 < z < d/2$:

$$a_y = (z-z_1)(z-3z_1+2z_\gamma) - (z_1-z_\gamma)^2\,, \qquad (A4)$$

for $x_2 < x < a$, $z_\gamma < z < d/2$:

$$a_y = (z - z_\gamma)^2\,. \qquad (A5)$$

For $-a < x < a$, $z \geq d/2$ (above the strip) one has

$$A_y(x,z) = A_y(x,d/2) - (J_c/2)F(x,h)(z - d/2). \quad (A6)$$

The appropriate expressions below the core follows from the symmetry relationship $A_y(x,-z) = -A_y(-x,z)$. Outside the core width one has for $x > a$ and all z inside or close to the strip [for $x < -a$ use $A_y(x,z) = -A_y(-x,-z)$]:

$$A_y(x,z) = A_y(a,0) + \int_a^x H_z(x',0)dx' - H_{ax}z$$
$$+ \frac{J_c}{2}g(x,z) \quad (A7)$$

where $A_y(a,0) = d\,H_{ax}^2/2J_c$, $g = z^2/d$ inside and $g = |z| - d/4$ outside the strip for $x < w$, $g = 0$ for $x > w$, and $H_z(x,0)$ from Ref. 12. Using formulas $\mathrm{arctanh}(1/u) = \mathrm{arctanh}(u) + i\pi/2$ (at $|u| < 1$) and $\mathrm{arctanh}(iu) = i\arctan(u)$, we may write one single expression valid for all $-\infty < x < \infty$ (Re means real part):

$$H_z(x,0) = \frac{J_c}{\pi}\mathrm{Re}\left\{\mathrm{arctanh}\sqrt{\frac{1-a^2/x^2}{1-a^2}}\right\}. \qquad (A8)$$

APPENDIX B: MAGNETIC MOMENT

From the general definition of the magnetic moment of the strip per unit length, $(M_x, M_z) = \int dx \int dz(-z,x)J_y(x,z)$, one obtains the following saturation values in the two limiting cases: For $H_a \geq H_p^\perp = (J_c/\pi)\ln(2ew/d)^{15}$ along z, one has $j(x,z) = -j_c\,\mathrm{sign}(x)$ and $M_z = M_z^{\mathrm{sat}} = -j_cdw^2 = -J_cw^2$. For $H_a \geq J_c/2$ along x, one has $j(x,z) = j_c\,\mathrm{sign}(z)$ and $M_x = M_x^{\mathrm{sat}} = -j_cd^2w/2 = -J_cdw/2$. The reduced magnetic moment $m_z = M_z/M_z^{\mathrm{sat}}$ along z depends only on $H_{az} = H_a\cos\theta$, and is given by Eq. (23). The magnetic moment along x, Eq. (24), in general depends on both components and has to be computed from the current fronts. Explicit formulas for $m_x = M_x/M_x^{\mathrm{sat}}$ can be obtain for any H_a, but here we present them only in the case $H_a \geq H_p = J_c/2\sin\theta$. Namely, for scenario 1 the formulas of Sec. II yield for $h \geq h_p$

$$m_x = \int_0^{x_1}dx\left[1 - \left(\frac{2}{\pi}\arctan\frac{x\sqrt{1-a^2}}{\sqrt{a^2-x^2}}\right)^2\right]$$
$$+ \int_{x_1}^a dx\left[1 - \frac{2}{\pi}\arctan\frac{x\sqrt{1-a^2}}{\sqrt{a^2-x^2}}\right] \times$$
$$\left[1 + \frac{2}{\pi}(h-h_*)\sin\theta + \frac{2}{\pi}\arctan\frac{\sqrt{\sin^2\theta-x^2}}{\cos\theta}\right], \quad (B1)$$

with $h_* = \mathrm{arcosh}(\sin\theta/x)/\cos\theta$, Eq. (9). For scenario 2 the formulas of Sec. III yield for $h \geq h_p$

$$m_x = \int_0^a dx\left[1 - \left(\frac{2}{\pi}\arctan\frac{x\sqrt{1-a^2}}{\sqrt{a^2-x^2}}\right)^2\right], \qquad (B2)$$

which does not depend on H_{ax}.

[1] M. V. Indenbom, C. J. van der Beek, V. Berseth, W. Benoit, G. D'Anna, A. Erb, E. Walker, R. Flükiger, Nature **385**, 702 (1994).
[2] M. V. Indenbom, A. Forkl, B. Ludescher, H. Kronmüller, H.-U. Habermeier, B. Leibold, G. D'Anna, T. W. Li, P. H. Kes, A. A. Menovsky, Physica C **226**, 325 (1994).
[3] A. A. Zhukov, G. K. Perkins, Yu. V. Bugoslavsky, A. D. Caplin, Phys. Rev. B **56**, 2809 (1997).
[4] K. Itaka, T. Shibauchi, M. Yasugaki, T. Tamegai, S. Okayasu, Phys. Rev. Lett. **86**, 5144 (2001).
[5] M. A. Avila, L. Civale, A. V. Silhanek, R. A. Ribeiro, O. F. de Lima, H. Lanza, Phys. Rev. B **64**, 144502 (2001).
[6] D. Karmakar, K. V. Bhagwat, Phys. Rev. B **65**, 024518 (2001).
[7] C. P. Bean, Phys. Rev. Lett. **8**, 250 (1962); Rev. Mod. Phys. **36**, 31 (1964).
[8] A. M. Campbell and J. E. Evetts, Adv. Phys. **21**, 199 (1972).
[9] G. P. Mikitik and E. H. Brandt, Phys. Rev. B **62**, 6800 (2000).
[10] E. H. Brandt and G. P. Mikitik, Phys. Rev. Lett. **89**, 027002 (2002).
[11] G. P. Mikitik, E. H. Brandt, Phys. Rev. B **67**, 104511 (2003).
[12] E. H. Brandt, M. Indenbom, A. Forkl, Europhys. Lett. **22**, 735 (1993).
[13] E. H. Brandt, M. Indenbom, Phys. Rev. B **48**, 12893 (1993).
[14] E. Zeldov, J. R. Clem, M. McElfresh, M. Darwin, Phys. Rev. B **49**, 9802 (1994).
[15] E. H. Brandt, Phys. Rev. B **54**, 4246 (1996).
[16] E. H. Brandt, Phys. Rev. B **49**, 9024 (1994).
[17] A detachment of the core from the surface, and the appearance of two straight lines separating regions with $j = \pm j_c$, occurs even in perpendicular field ($\theta = 0$) when the applied field is so large that the core width $2a$ becomes smaller than

the strip thickness d, namely, at $H_a \approx 0.5H_p^\perp - H_p^\perp$ where $H_p^\perp = (J_c/\pi)\ln(2ew/d)$ is the field of full penetration of a perpendicular field[15], see Fig. 2 in Ref. 15. In contrast, our present result for $\theta \gg d/w$ yields core detachment at

arbitrarily large core width.

[18] C. Y. Pang, A. M. Campbell, P. G. MacLaren, IEEE Trans. Magn. **17**, 134 (1981).